Synthesis and structural characterization of metallacarborane sandwich salts with tetrathiafulvalene (ttf) $[M(C_2B_9H_{11})_2][ttf]$ (M = Cr, Fe, Ni)

Jennifer M. Forward [a], D. Michael P. Mingos [b], Thomas E. Müller [b], David J. Williams [b] and Yaw-Kai Yan [b]

[a] *Inorganic Chemistry Laboratory, University of Oxford, South Parks Road, Oxford OX1 3QR (UK)*
[b] *Department of Chemistry, Imperial College of Science, Technology and Medicine, South Kensington, London SW7 2AY (UK)*

(Received June 21, 1993)

Abstract

Tetrathiafulvalenium ($ttf^{\cdot+}$) salts of the metallacarborane anions *commo*-$[3,3'\text{-}M(1,2\text{-}C_2B_9H_{11})_2]^-$ (**1**, M = Cr; **2**, M = Fe; **3**, M = Ni) were synthesized for a study of their magnetic properties. They are complementary to the magnetic charge-transfer salts based on decamethylmetallocenes previously studied by others. X-Ray crystallographic analysis revealed that the molecular packing in **1** consists of alternating layers of $ttf^{\cdot+}$ radical cations and $[Cr(C_2B_9H_{11})_2]^-$ anions. In contrast, the crystal structures of **2** and **3**, which are isomorphous, comprise three-dimensional herring-bone networks of the corresponding metallacarborane anions, with stacked dimers of $ttf^{\cdot+}$ cations occupying cavities in the network. The interplanar separation between the fully eclipsed $ttf^{\cdot+}$ radical cations in each dimer is 3.4 Å, indicating significant bonding interactions between the radical cations. There are otherwise no intermolecular distances shorter than van der Waals contacts in any of the salts **1–3**. Variable-temperature magnetic susceptibility measurements were performed on the title compounds down to 6 K. The susceptibility data fit the Curie–Weiss law for systems containing non-interacting unpaired spins, with small values of θ ($\theta = -2.5$ K for **1**; $\theta = -2.0$ K for **2** and $\theta = +1.5$ K for **3**).

Key words: Metallacarborane; Iron; Nickel; Chromium; Tetrathiafulvalene; Magnetic

1. Introduction

Low-dimensional ionic molecular solids have been the subject of intense research activity for over two decades because in many cases they exhibit interesting electrical [1] and magnetic properties [2]. Co-operative magnetic phenomena, for example, have been observed in a series of salts containing $S \geq 1/2$ decamethylmetallocene cations and planar polycyano-organic radical anions [2]. Miller and co-workers rationalized the magnetic behaviour of these salts using the extended-McConnell configurational admixture model [3]. Although this model is useful in explaining and predicting the magnetic properties of the Miller-type salts, its assumptions and its general validity have been questioned [4].

In an attempt to further test the extended-McConnell model and to establish a new class of molecular magnetic materials, it was decided to synthesize and study several molecular salts incorporating metallacarborane sandwich complexes of the *nido*-$[7,8\text{-}C_2B_9H_{11}]^{2-}$ ligand. The chemical behaviour of these complexes has been widely studied by Hawthorne [5], but their potential in this area of molecular electronics has not previously been examined. The metallacarborane complexes have the advantage of being more stable [6] than the corresponding metallocene analogues, with which they are isoelectronic. The existence of the negatively charged metallacarborane sandwich compounds enables studies of charge transfer salts with planar radical cations, such studies being complementary to those by Miller which involved cationic sandwich compounds and anionic organic radicals. Although the molecular volumes of the metallacarborane complexes remain very close to those of the decameth-

Correspondence to: Professor D.M.P. Mingos.

0022-328X/94/$7.00
SSDI 0022-328X(93)24046-8

ylmetallocenes [7] they exhibit a wider range of stable oxidation states [6] and are more prolate in shape than the metallocenes. The packing of prolate ions in a regular fashion within the crystal may lead to alignments that enhance the magnetic interactions. The possible formation of charge-transfer salts containing stacked organic donor molecules in mixed oxidation states is also of interest since such salts may show novel conducting properties.

In this paper, we describe the synthesis, crystal structures, and the spectroscopic and magnetic properties of tetrathiafulvalenium ($ttf^{\cdot+}$) salts of the metallacarborane anions *commo*-[3,3′-M(1,2-$C_2B_9H_{11})_2]^-$ (M = Cr^{III}, Fe^{III}, Ni^{III}). These compounds are the first organic donor-metallacarborane hybrid salts.

2. Results and discussion

2.1. Synthesis of $[ttf]^{\cdot+}[M(C_2B_9H_{11})_2]^-$ *(1, M = Cr; 2, M = Fe; 3, M = Ni)*

The commonly employed method of preparing $ttf^{\cdot+}$ salts, involving metathetical reaction with $[ttf]_3[BF_4]_2$ in acetonitrile [8], proved not to be feasible for the preparation of the charge transfer salts **1–3** based on metallacarborane sandwich anions because the resulting salts are more soluble in acetonitrile than $[ttf]_3[BF_4]_2$. The

TABLE 1. Crystal and refinement data for compounds **1–3**

Compound	**1** $[ttf]^{\cdot+}[Cr(C_2B_9H_{11})_2]^-$	**2** $[ttf]^{\cdot+}[Fe(C_2B_9H_{11})_2]^-$	**3** $[ttf]^{\cdot+}[Ni(C_2B_9H_{11})_2]^-$
(a) Crystal data			
Chemical formula	$C_{10}H_{26}B_{18}CrS_4$	$C_{10}H_{26}B_{18}FeS_4$	$C_{10}H_{26}B_{18}NiS_4$
FW	521.1	525.0	527.8
Crystal system	Monoclinic	Monoclinic	Monoclinic
Unit cell dimensions			
a (Å)	9.971(2)	11.737(3)	11.251(5)
b (Å)	10.325(2)	20.471(5)	20.477(8)
c (Å)	12.617(2)	11.241(3)	11.765(6)
β (°)	102.64(2)	115.15(2)	115.79(2)
V (Å^3)	1267.5(5)	2445.0(7)	2440(2)
Space group	$C2$ [a]	$P2_1/n$	$P2_1/n$
D_c (g cm^{-3})	1.365	1.426	1.437
Z	2	4	4
F(000)	528	1064	1072
Colour, habit	Black prisms	Black prisms	Black prisms
Crystal dimensions (mm)	0.30 × 0.36 × 0.46	0.86 × 0.44 × 0.26	0.13 × 0.23 × 0.57
μ (mm^{-1})	0.782(Mo Kα)	8.097(Cu Kα)	1.139(Mo Kα)
(b) Data collection and processing			
Diffractometer	Siemens P4/PC	Nonius CAD4	Siemens P4/PC
X-Radiation	Mo Kα	Cu Kα	Mo Kα
Scan mode	ω	ω–2θ	ω
ω-scan width (°)	0.90	0.62 + 0.15 tan θ	0.90
2θ limits (°)	3.0–70.0	0.0–144.0	4.0–50.0
Min, max h, k, l	0,16; 0,16; −20,19	−14,14; −1,25; −1,13	0,13; 0,24; −14,12
No of reflections			
Total	3040	6068	4510
Unique (R_{int}/%)	2924 (1.67)	4780 (4.25)	4285 (2.46)
Observed	2473	3131	2831
	[$\lvert F_o \rvert \geq 4\sigma(\lvert F_o \rvert)$]	[$I > 3\sigma(I)$]	[$\lvert F_o \rvert \geq 4\sigma \lvert (F_o \rvert)$]
Absorption correction	N/A	DIFABS	N/A
Min, max corrections	N/A	0.642, 1.658	N/A
(c) Structure analysis and refinement			
No. of parameters	152	301	301
Weighting scheme	$w^{-1} = \sigma^2(F) + 0.0005F^2$	Chebychev (3 parameters: 7.40, −2.65, 5.98)	$w^{-1} = \sigma^2(F) + 0.0005F^2$
R (observed data) (%)	3.11	4.13	4.38
R_w (observed data) (%)	3.35	4.66	4.03

[a] The polarity of the structure was determined by an R-factor test.

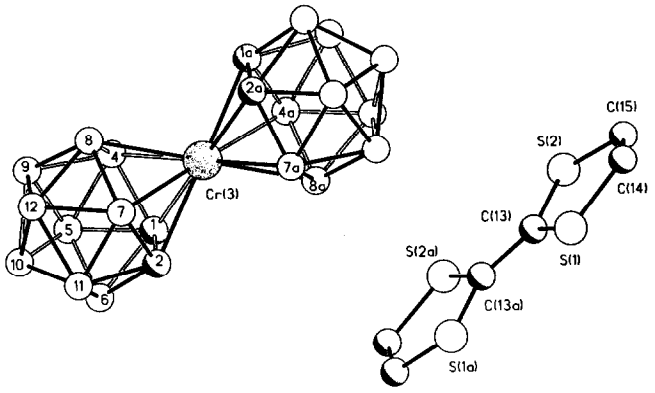

Fig. 1. The molecular structures of the cation and anion in $[ttf]^{\cdot+}[Cr(C_2B_9H_{11})_2]^-$ (1) showing the atomic labelling scheme.

metallacarboranes with the metal ions in a formal oxidation state of +3 were chosen, and with d^3, d^5 and d^7 electronic configurations in order to provide a range of possible spin states.

The salts **1**, **2** and **3** are all black crystalline solids, which are soluble in polar organic solvents such as acetone and acetonitrile, but sparingly soluble in ethanol. They are all air-stable solids. The charge transfer salts **1** and **2** were prepared by metathesis of [ttf]Cl with $Cs[Cr(C_2B_9H_{11})_2]$ or $Na[Fe(C_2B_9H_{11})_2]$, respectively, in water. Only one product was isolated in each case. Single crystals of **1** and **2** suitable for X-ray analysis were obtained by slow evaporation of solutions in acetone/ethanol mixtures.

The corresponding nickelacarborane charge-transfer salt **3** was obtained as large black crystals by the slow evaporation of a CH_2Cl_2/n-hexane (1 : 1) solution containing neutral ttf and the Ni(IV) complex *commo*-[3,3′-$Ni(C_2B_9H_{11})_2$] in equimolar quantities. As in the preparation of **1** and **2**, no other ttf-metallacarborane salt was formed.

2.2. *Crystal structure of* $[ttf]^{\cdot+}[Cr(C_2B_9H_{11})_2]^-$ *(1)*

The molecular structures of the cation and anion in **1** are shown in Fig. 1. Both the anion and cation have crystallographic C_2 symmetry. In the cation, the two-fold axis passes through the centre of the C(13)–C(13a) bond and lies in the plane of the four sulfur atoms.

The $[Cr(C_2B_9H_{11})_2]^-$ anion, the structure of which has not previously been determined by X-ray analysis, shows the staggered sandwich structure with the carbon atoms of the two C_2B_9 cages adopting an essentially *anti* geometry with respect to the Cr centre. The upper and lower C_2B_3 rings are rotated by *ca.* 179° with respect to each other about an axis between their centroids. The centroid-centroid vector is perpendicular to both C_2B_3 planes. The distance of the Cr atom from each C_2B_3 plane is 1.69 Å. The C_2B_3 bonding faces are parallel and planar, with a maximum deviation of 0.01 Å from the mean plane [for B(8)]. The bond lengths and angles in the molecule are similar to those in $Cs^+[Cr\{C_2B_9H_9(CH_3)_2\}_2]^-$ [9] except that the Cr–C bonds in **1** [2.185(6) and 2.205(4) Å] are significantly shorter than those in $Cs^+[Cr\{C_2B_9H_9(CH_3)_2\}_2]^-$ [2.262(7) and 2.272(7) Å].

The bond lengths within the $[ttf]^{\cdot+}$ unit (see Table 3) are very close to those in $[ttf]^{\cdot+}[ClO_4]^-$ [10]. This provides evidence that the ttf molecules are in the 1 + oxidation state. The $[ttf]^{\cdot+}$ cation is not planar, since there is a dihedral angle of 1.6° between the mean planes of the pentagonal halves of the ion. There is, however, no twist about the C(13)–C(13a) bond.

The packing of the molecules in the crystal (Fig. 2) shows the cations to lie on one two-fold axis and the anions on another. The lattice consists of chains of alternating $[ttf]^{\cdot+}$ and $[Cr(C_2B_9H_{11})_2]^-$ ions which extend in the *c*-direction. The crystal structure may also be described in terms of alternating layers of $[ttf]^{\cdot+}$ and $[Cr(C_2B_9H_{11})_2]^-$ ions. No intermolecular bonding

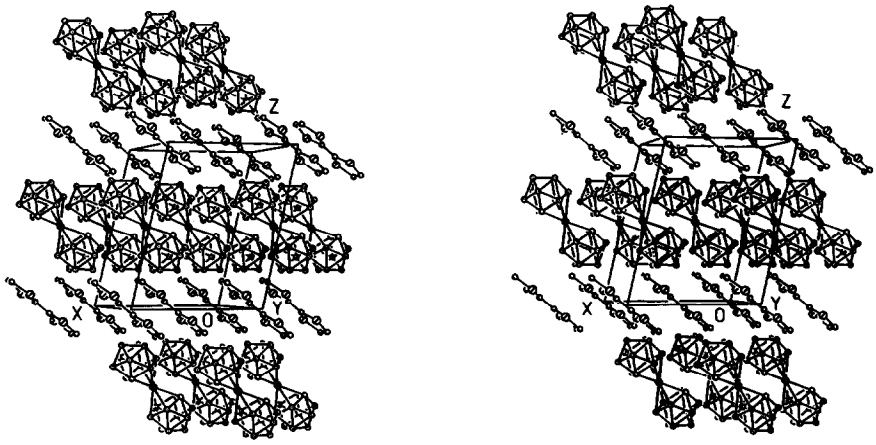

Fig. 2. Stereoscopic view of the packing of ions in crystals of **1**.

TABLE 2. Atomic coordinates ($\times 10^4$) and equivalent isotropic displacement coefficients ($Å^2 \times 10^3$) for **1**

Atom	x	y	z	U_{eq} [a]
Cr(3)	10000	−1400	15000	26(1)
C(1)	12078(6)	−2163(5)	15563(4)	42(2)
C(2)	12084(4)	−603(4)	15579(3)	25(1)
B(4)	10989(6)	−2737(6)	16327(5)	31(1)
B(5)	12834(6)	−2756(8)	16860(5)	49(2)
B(6)	13502(2)	−1469(10)	16333(2)	41(1)
B(7)	11004(6)	−7(6)	16290(4)	28(1)
B(8)	10286(2)	−1391(7)	16825(1)	28(1)
B(9)	11670(7)	−2278(5)	17661(5)	34(1)
B(10)	13234(2)	−1380(11)	17670(2)	45(1)
B(11)	12773(6)	12(6)	16812(4)	35(1)
B(12)	11667(6)	−560(6)	17649(4)	34(1)
S(1)	8520(2)	9(2)	9161(1)	39(1)
S(2)	8524(2)	−2796(2)	9158(1)	39(1)
C(13)	9356(2)	−1379(6)	9636(1)	29(1)
C(14)	7099(6)	−777(7)	8407(6)	50(2)
C(15)	7123(5)	−2055(5)	8341(5)	40(1)

[a] Equivalent isotropic U defined as one-third of the trace of the orthogonalized U_{ij} tensor.

interactions are evident between the $[ttf]^{\cdot+}$ ions, the closest intermolecular S · · · S contact being 3.96 Å. There are also no close C · · · S contacts.

Adjacent anions are packed in such a way that each approximately spherical $[C_2B_9H_{11}]$ fragment of one molecule occupies the cleft between the two $[Cr(C_2B_9H_{11})_2]^-$ units adjacent to it. No short contact is observed between the Cr atom of one anion and any atom of another anion, the shortest intermolecular distance being 4.20 Å between Cr(3) and the hydrogen attached to B(11).

There are also no short contacts between the cations and anions. The shortest intrachain Cr · · · S distances are 5.93 and 5.94 Å, and the shortest distance between a ttf sulfur atom and a hydrogen on the C_2B_3 bonding ring is 3.29 Å [S(1) to H on B(8)]. The shortest interchain Cr · · · S distances are 6.75 and 6.76 Å.

TABLE 3. Selected bond lengths (Å), and angles (°) in **1**

S(1)–C(13)	1.700(5)	Cr(3)–B(4)	2.227(6)
S(1)–C(14)	1.727(6)	Cr(3)–B(7)	2.238(5)
S(2)–C(13)	1.725(5)	Cr(3)–B(8)	2.257(2)
S(2)–C(15)	1.723(5)	C(1)–C(2)	1.610(7)
C(13)–C(13a)	1.406(3)	C(1)–B(4)	1.709(9)
C(14)–C(15)	1.323(9)	C(2)–B(7)	1.662(7)
Cr(3)–C(1)	2.185(6)	B(4)–B(8)	1.735(9)
Cr(3)–C(2)	2.205(4)	B(7)–B(8)	1.795(8)
C(1)–C(2)–B(7)	112.1(4)	C(1)–Cr(3)–C(2a)	179.1(2)
C(2)–B(7)–B(8)	105.5(4)	C(2)–Cr(3)–C(1a)	179.1(2)
B(4)–B(8)–B(7)	106.0(3)	B(4)–Cr(3)–B(7a)	178.0(2)
C(1)–B(4)–B(8)	106.4(4)	B(7)–Cr(3)–B(4a)	178.0(2)
C(2)–C(1)–B(4)	109.9(4)	B(8)–Cr(3)–B(8a)	179.5(5)

2.3. Crystal structure of $[ttf]^{\cdot+}[Fe(C_2B_9H_{11})_2]^-$ (2)

The structures of the cation and anion in **2** are shown in Fig. 3, together with the atomic labelling scheme.

The C_2B_9 cages of the anion are staggered and in a cisoid arrangement, with the carbon atoms of different cages at a minimum distance apart; *cf.* the transoid conformation in $[Cr(C_2B_9H_{11})_2]^-$ (*vide supra*) and $[Fe(C_2B_9H_{11})_2]^{2-}$ [11]. Here the two C_2B_3 rings are rotated by *ca.* 36° with respect to each other about their centroid–centroid axis. The distance of the Fe atom from each C_2B_3 plane is 1.53 Å. This distance is close to that observed in $[Fe(C_2B_9H_{11})_2]^{2-}$ (1.48 Å) [11], suggesting that the HOMO of $[Fe(C_2B_9H_{11})_2]^{2-}$ is essentially non-bonding in character. Both C_2B_3 bonding faces are nearly planar, each with a maximum deviation of 0.01 Å from the mean plane [for B(4) and B(8′), respectively]. The two faces are also not parallel, being inclined by *ca.* 3° to each other.

The bond lengths within the ttf unit (see Table 5) are consistent with the 1+ oxidation state of the molecule. The $[ttf]^{\cdot+}$ cation adopts a twist-boat conformation, with a twist of 1.6° about the C(13)–C(13′) bond and a dihedral angle of 3.4° between the mean planes of the two pentagonal rings of the ion.

The packing diagram for **2** is shown in Fig. 4. In contrast to **1**, discrete stacked dimers of $[ttf]^{\cdot+}$ cations occur in the crystal structure of **2**. The dimers occupy cavities in a three-dimensional herring-bone network of $[Fe(C_2B_9H_{11})_2]^-$ anions, with each dimer having 12 nearest anionic neighbours. The main component of

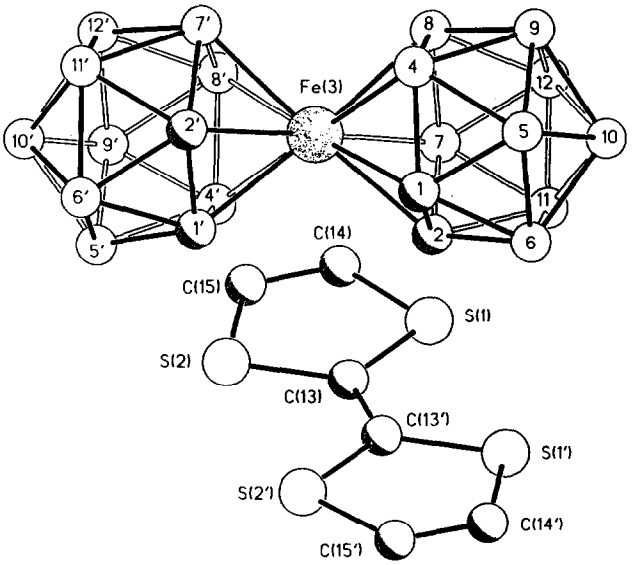

Fig. 3. Diagram of the molecular structures of the cation and anion in $[ttf]^{\cdot+}[Fe(C_2B_9H_{11})_2]^-$ (**2**) showing the atomic labelling scheme.

TABLE 4. Atomic coordinates ($\times 10^4$) and equivalent isotropic displacement coefficients ($Å^2 \times 10^3$) for **2**

Atom	x	y	z	U_{iso}
Fe(3)	0.22271(4)	0.21428(2)	0.17747(4)	0.0241
C(1)	0.0779(3)	0.2828(2)	0.1353(3)	0.0335
C(2)	0.0937(3)	0.2351(2)	0.2559(3)	0.0353
B(4)	0.2160(4)	0.3174(2)	0.1570(3)	0.0354
B(5)	0.0974(4)	0.3628(2)	0.1809(4)	0.0435
B(6)	0.0158(4)	0.3083(2)	0.2401(4)	0.0417
B(7)	0.2445(4)	0.2335(2)	0.3719(4)	0.0369
B(8)	0.3282(3)	0.2877(2)	0.3129(4)	0.0381
B(9)	0.2563(4)	0.3671(2)	0.2984(4)	0.0424
B(10)	0.1326(4)	0.3614(2)	0.3510(4)	0.0416
B(11)	0.1251(4)	0.2789(2)	0.3950(4)	0.0404
B(12)	0.2733(4)	0.3144(2)	0.4304(4)	0.0397
C(1')	0.1306(3)	0.1399(1)	0.0454(3)	0.0335
C(2')	0.2028(3)	0.1894(2)	−0.0111(3)	0.0391
B(4')	0.2257(3)	0.1114(2)	0.1949(4)	0.0339
B(5')	0.1815(4)	0.0609(2)	0.0531(4)	0.0407
B(6')	0.1642(4)	0.1129(2)	−0.0796(4)	0.0397
B(7')	0.3575(4)	0.1982(2)	0.0997(4)	0.0402
B(8')	0.3767(3)	0.1461(2)	0.2359(4)	0.0382
B(9')	0.3387(4)	0.0644(2)	0.1714(4)	0.0410
B(10')	0.3027(4)	0.0657(2)	0.0000(4)	0.0440
B(11')	0.3133(4)	0.1483(2)	−0.0436(4)	0.0431
B(12')	0.4222(3)	0.1186(2)	0.1112(4)	0.0425
S(1)	0.77476(8)	−0.06807(5)	0.36000(9)	0.0467
S(2)	0.80822(9)	0.01808(4)	0.57604(9)	0.0468
C(13)	0.8693(3)	−0.0431(1)	0.5171(3)	0.0360
C(14)	0.6539(3)	−0.0163(2)	0.3394(4)	0.0545
C(15)	0.6680(4)	0.0239(2)	0.4385(5)	0.0556
S(1')	1.04573(9)	−0.13176(4)	0.5256(1)	0.0493
S(2')	1.08073(9)	−0.04912(5)	0.74804(9)	0.0499
C(13')	0.9862(3)	−0.0715(2)	0.5890(3)	0.0375
C(14')	1.1818(4)	−0.1426(2)	0.6669(5)	0.0604
C(15')	1.1974(4)	−0.1047(2)	0.7677(4)	0.0571

TABLE 5. Selected bond lengths (Å) and angles (°) in **2**

S(1)–C(13)	1.716(3)	Fe(3)–C(1')	2.080(3)
S(1)–C(14)	1.706(4)	Fe(3)–C(2')	2.095(3)
S(2)–C(13)	1.711(3)	Fe(3)–B(4')	2.114(3)
S(2)–C(15)	1.718(4)	Fe(3)–B(7')	2.134(4)
C(13)–C(13')	1.390(5)	Fe(3)–B(8')	2.154(4)
C(14)–C(15)	1.338(6)	C(1)–C(2)	1.617(4)
S(1')–C(13')	1.715(3)	C(1)–B(4)	1.689(5)
S(1')–C(14')	1.723(5)	C(2)–B(7)	1.695(5)
S(2')–C(13')	1.718(3)	B(4)–B(8)	1.793(5)
S(2')–C(15')	1.721(5)	B(7)–B(8)	1.787(5)
C(14')–C(15')	1.320(7)	C(1')–C(2')	1.614(4)
Fe(3)–C(1)	2.096(3)	C(1')–B(4')	1.678(5)
Fe(3)–C(2)	2.094(3)	C(2')–B(7')	1.721(5)
Fe(3)–B(4)	2.122(4)	B(4')–B(8')	1.779(5)
Fe(3)–B(7)	2.127(4)	B(7')–B(8')	1.799(6)
Fe(3)–B(8)	2.123(4)		
C(1)–C(2)–B(7)	111.6(2)	B(9)–B(8)–B(12)	59.2(2)
C(2)–B(7)–B(8)	105.1(2)	B(5)–C(1)–B(6)	62.7(2)
B(4)–B(8)–B(7)	106.4(3)	B(6)–C(2)–B(11)	62.3(2)
C(1)–B(4)–B(8)	105.1(2)	B(11)–B(7)–B(12)	59.7(2)
C(2)–C(1)–B(4)	111.8(2)	B(5)–B(4)–B(9)	59.7(2)
B(5)–B(6)–B(11)	107.5(3)	C(1)–Fe(3)–C(2')	101.7(1)
B(6)–B(11)–B(12)	108.3(3)	C(2)–Fe(3)–C(1')	101.6(1)
B(9)–B(12)–B(11)	108.1(3)	B(4)–Fe(3)–B(7')	96.3(1)
B(5)–B(9)–B(12)	107.6(3)	B(7)–Fe(3)–B(4')	95.7(1)
B(6)–B(5)–B(9)	108.4(3)	B(8)–Fe(3)–B(8')	94.7(1)

the network of anions are chains that extend in the (101) direction.

The $[ttf]^{\cdot+}$ cations within the dimers are centrosymmetrically related and are fully eclipsed, with an interplanar separation of 3.44 Å. Short intradimer S · · · S contacts of 3.44 Å [S(1) · · · S(2'a)] and 3.37 Å [S(2) · · · S(1'a)] indicate significant bonding interactions between the ions making up the dimers [1a,b]. There are no interdimer interactions, the shortest interdimer S · · · S distance being 6.73 Å.

2.4. Crystal structure of $[ttf]^{\cdot+}[Ni(C_2B_9H_{11})_2]^-$ (3)

Crystals of **3** are isomorphous with those of **2**. (It should be noted that the *a* and *c* axes are interchanged between the two structures.) The gross structural features of **3** are thus essentially the same as those of **2**. A few features of the present structure are, however, noteworthy. The $[Ni(C_2B_9H_{11})_2]^-$ anion adopts a cisoid conformation in **3**, whilst it adopts the transoid conformation in its tetramethylammonium salt [12]. Whereas the C_2B_3 faces in the latter salt are parallel, those in **3** are inclined by 5.3° to each other. The distance of the Ni atom from each C_2B_3 plane is 1.54

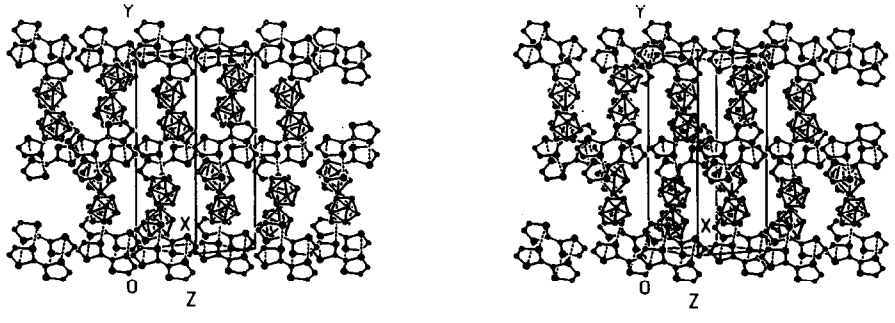

Fig. 4. Stereoscopic view of the molecular packing of **2** down the (1 0 −1) direction.

Å. Although the face defined by C(1'), C(2'), B(4'), B(7') and B(8') in **3** (see Fig. 5) is planar within experimental error, the opposite C_2B_3 face is significantly distorted, with a maximum deviation from the mean plane of 0.02 Å [for C(1)]. The extent of folding of the latter face cannot be properly described by the angles ϕ and θ as defined in ref. 13 because the fold is along the imaginary line joining C(2) and B(4) rather than that joining B(4) and B(7). The angles made by the planes C(1)–C(2)–B(4) and C(2)–B(4)–B(7)–B(8) to the plane B(5)–B(6)–B(9)–B(11)–B(12) are 3.3° and 1.0°, respectively. In addition, two of the Ni–B bonds in **3** are apparently strengthened at the expense of two of the Ni–C bonds [Ni(3)–B(8) = 2.108(5) Å, Ni(3)–B(8') = 2.116(5) Å, Ni(3)–C(1) = 2.151(6) Å, Ni(3)–C(1') = 2.123(5) Å]. A similar phenomenon was observed in $[Me_4N]^+[Ni(C_2B_9H_{11})_2]^-$, in which the Ni–C bonds are all 2.15 Å long, four of the Ni–B bonds are 2.11 Å long and the remaining two Ni–B bonds are 2.16 Å long [12]. This is in accord with the general observation that metal–boron bonds are strengthened at the expense of metal–carbon bonds in electron-rich metallacarboranes. The subtle differences between the structures of the nickelacarborane anion in **3** and in $[Me_4N]^+[Ni(C_2B_9H_{11})_2]^-$ imply that the anion is sufficiently flexible to fine-tune its conformation to suit the particular environment found in the crystal structure.

It is noteworthy that the molecular packing observed in **2** and **3** differs drastically from that observed in **1**. An attempt to grow crystals of **2** which are isomorphous to **1** by seeding an acetone/ethanol solution of **2** with microcrystals of **1** was unsuccessful. The significantly lower density of crystals of **1** (1.365 g cm^{-3}) compared to those of **2** (1.426 g cm^{-3}) and **3** (1.437 g cm^{-3}) implies that the molecular packing in **1** is less efficient than that in **2** and **3**. In an attempt to understand why the packing in **1** differs from that in **2** and **3**, the molecular volumes, V_m, and the moments of inertia, M_1, M_2 and M_3 ($M_1 \geq M_2 \geq M_3$) of the metallacarborane anions in **1**, **2** and **3** were calculated using the methods described in ref. 14. The results are tabulated in Table 8. It can be seen that, whilst the molecular volumes of the three anions are very similar, the $[Cr(C_2B_9H_{11})_2]^-$ anion is significantly more prolate than its iron and nickel analogues. The greater prolateness of the chromacarborane anion is reflected in the lower dimensionality of the molecular packing in **1**, in which the anions form sheets rather than the three-dimensional networks observed in **2** and **3**.

TABLE 6. Atomic coordinates ($\times 10^4$) and equivalent isotropic displacement coefficients ($Å^2 \times 10^3$) for **3**

Atom	x	y	z	U_{eq} [a]
Ni(3)	1762(1)	2147(1)	2199(1)	23(1)
C(1)	2583(4)	2367(2)	898(4)	30(2)
C(2)	1359(4)	2832(2)	754(4)	32(2)
B(4)	3710(5)	2330(3)	2391(5)	29(2)
B(5)	3965(5)	2808(3)	1238(5)	35(2)
B(6)	2408(6)	3092(3)	127(5)	40(2)
B(7)	1537(5)	3192(2)	2100(5)	31(2)
B(8)	3097(5)	2883(3)	3253(5)	32(2)
B(9)	4291(5)	3141(3)	2724(5)	35(2)
B(10)	3502(5)	3619(3)	1311(5)	37(2)
B(11)	1804(5)	3635(3)	930(5)	37(2)
B(12)	2952(5)	3676(3)	2530(5)	36(2)
C(1')	−137(4)	1890(2)	2028(4)	32(2)
C(2')	433(4)	1392(2)	1297(4)	28(2)
B(4')	971(5)	1992(3)	3536(5)	33(2)
B(5')	−439(6)	1472(3)	3138(5)	37(2)
B(6')	−806(5)	1120(3)	1655(5)	34(2)
B(7')	1922(5)	1102(2)	2203(5)	27(2)
B(8')	2368(5)	1477(3)	3717(5)	32(2)
B(9')	1150(6)	1210(3)	4204(5)	41(3)
B(10')	36(6)	666(3)	3048(5)	41(3)
B(11')	521(6)	605(3)	1819(5)	38(2)
B(12')	1725(6)	659(3)	3370(5)	40(2)
S(1)	−239(1)	3677(1)	−5440(1)	46(1)
S(2)	−2492(1)	4495(1)	−5837(1)	48(1)
C(13)	−887(4)	4280(2)	−4865(4)	34(2)
C(14)	−1649(6)	3559(3)	−6795(5)	60(3)
C(15)	−2669(6)	3933(3)	−6974(5)	58(3)
S(1')	1405(1)	4331(1)	−2738(1)	43(1)
S(2')	−782(1)	5182(1)	−3110(1)	45(1)
C(13')	−173(4)	4572(2)	−3704(4)	30(2)
C(14')	1596(6)	4853(3)	−1542(5)	53(3)
C(15')	597(6)	5243(3)	−1709(5)	50(3)

[a] Equivalent isotropic U defined as one-third of the trace of the orthogonalized U_{ij} tensor.

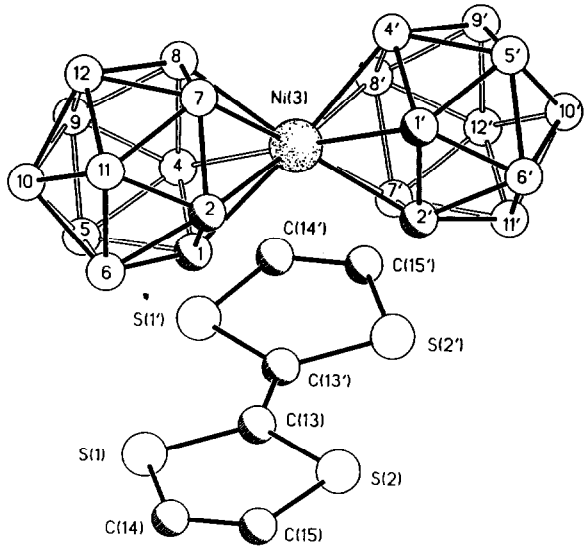

Fig. 5. Diagram of the molecular structures of the cation and anion in $[ttf]^{\cdot+}[Ni(C_2B_9H_{11})_2]^-$ (**3**) showing the atomic labelling scheme.

TABLE 7. Selected bond lengths (Å) and angles (°) in **3**

S(1)–C(13)	1.717(6)	Ni(3)–C(1′)	2.123(5)
S(1)–C(14)	1.708(5)	Ni(3)–C(2′)	2.091(4)
S(2)–C(13)	1.722(4)	Ni(3)–B(4′)	2.142(7)
S(2)–C(15)	1.709(7)	Ni(3)–B(7′)	2.148(5)
C(13)–C(13′)	1.384(6)	Ni(3)–B(8′)	2.116(5)
C(14)–C(15)	1.319(10)	C(1)–C(2)	1.622(7)
S(1′)–C(13′)	1.712(4)	C(1)–B(4)	1.661(6)
S(1′)–C(14′)	1.704(6)	C(2)–B(7)	1.677(8)
S(2′)–C(13′)	1.713(5)	B(4)–B(8)	1.842(9)
S(2′)–C(15′)	1.707(5)	B(7)–B(8)	1.803(7)
C(14′)–C(15′)	1.322(9)	C(1′)–C(2′)	1.634(7)
Ni(3)–C(1)	2.151(6)	C(1′)–B(4′)	1.679(6)
Ni(3)–C(2)	2.096(5)	C(2′)–B(7′)	1.656(6)
Ni(3)–B(4)	2.136(6)	B(4′)–B(8′)	1.828(9)
Ni(3)–B(7)	2.151(5)	B(7′)–B(8′)	1.799(8)
Ni(3)–B(8)	2.108(5)		
C(1)–C(2)–B(7)	114.3(3)	B(5)–C(1)–B(6)	62.7(3)
C(2)–B(7)–B(8)	103.5(4)	B(6)–C(2)–B(11)	62.3(4)
B(4)–B(8)–B(7)	106.0(4)	B(11)–B(7)–B(12)	59.8(3)
C(1)–B(4)–B(8)	104.9(3)	B(9)–B(8)–B(12)	59.9(3)
C(2)–C(1)–B(4)	111.1(4)	B(5)–B(4)–B(9)	59.2(3)
B(5)–B(6)–B(11)	107.4(4)	C(1)–Ni(3)–C(2′)	103.1(2)
B(6)–B(11)–B(12)	109.0(4)	C(2)–Ni(3)–C(1′)	103.6(2)
B(9)–B(12)–B(11)	107.0(4)	B(4)–Ni(3)–B(7′)	95.3(2)
B(5)–B(9)–B(12)	108.0(3)	B(7)–Ni(3)–B(4′)	96.3(2)
B(6)–B(5)–B(9)	108.5(4)	B(8)–Ni(3)–B(8′)	94.7(2)

2.5. *Infrared spectra*

The infrared spectral data for the salts **1–3**, recorded as KBr pellets, are summarized in Table 9. The IR absorptions of both the $ttf^{\cdot+}$ cations [15] and the metallacarborane anions [5] are clearly represented in all the three spectra.

The occurrence of the b_{1u} (ν_{16}) absorption in the 825–830 cm^{-1} region in all the spectra is diagnostic of the presence of the radical cation $ttf^{\cdot+}$ in **1–3** [15]. The presence of $(ttf^{\cdot+})_2$ dimers in **2** and **3** is indicated by the high intensity of the $a_g(\nu_3)$ and $a_g(\nu_6)$ bands [15] in their spectra. These bands occur at 1353 and 493 cm^{-1}, respectively, in the spectrum of **2** and at 1358 and 493 cm^{-1}, respectively, in the spectrum of **3**. The a_g absorptions in the spectrum of **1** (at 1356 and 492 cm^{-1}, respectively) are much less intense. This is consistent with the absence of $(ttf^{\cdot+})_2$ dimers [15] in the crystal structure of **1**.

TABLE 8. Volumes and moments of inertia [a] of anions in compounds **1–3**

Anion	$[Cr(C_2B_9H_{11})_2]^-$	$[Fe(C_2B_9H_{11})_2]^-$	$[Ni(C_2B_9H_{11})_2]^-$
V_m (Å^3)	277.0	277.2	270.8
M_1 (Å^2)	361	327	329
M_2 (Å^2)	82	85	82
M_3 (Å^2)	80	83	80

[a] Moments of inertia were calculated without mass weighting.

TABLE 9. Infrared spectral data for compounds **1–3**

Compound	ν_{max} (cm^{-1})
1	3089s, 3072s, 3017m, 2531vs(br), 1505w, 1475s, 1356m, 1259m, 1085m, 1022w, 969s, 825s, 691s, 647s, 572m, 492w, 462w
2	3083s, 3029m, 2544vs(br), 1500w, 1470m, 1353vs, 1257m, 1090s, 975s, 829m, 748m, 719m, 687s, 493s, 463w
3	3083s, 3073s, 3038s, 2560vs(br), 1470m, 1358vs, 1256s, 1086s, 1012w, 968s, 867w, 830m, 749s, 696s, 493s, 454w

2.6. *UV-visible spectra*

The UV-visible spectral data for compounds **1–3** in acetonitrile solution are summarized in Table 10. For compounds **1** and **2**, the spectra are virtually superpositions of the UV-visible spectra of the constituent ions [5,16], thereby providing further support for the oxidation state assignments based on the structural and infrared data.

Interestingly, the electronic spectrum of **3** indicates that in solution, only the neutral species ttf [16] and $[Ni(C_2B_9H_{11})_2]$ [5b] are present. Correspondingly, **3** is soluble in relatively less polar solvents like CH_2Cl_2 and $CHCl_3$, giving yellow solutions from which ttf and $[Ni(C_2B_9H_{11})_2]$ may be separated by thin-layer chromatography.

That the neutral components ttf and $[Ni(C_2B_9H_{11})_2]$ are favoured in solution is consistent with the more positive reduction potential of $ttf^{\cdot+}$ ($E_{1/2}$ *vs.* SCE in CH_3CN = 0.33 V) [17] compared to $[Ni(C_2B_9H_{11})_2]$ ($E_{1/2}$ *vs.* SCE in CH_3CN = 0.25 V) [5b]. The preference for the ionic form $[ttf]^{\cdot+}$ $[Ni(C_2B_9H_{11})_2]^-$ in the crystalline state is most probably due to the additional lattice energy stabilization for the ionic form.

2.7. *Magnetic properties*

At 6 K the magnetizations of all the compounds **1–3** increase rapidly and linearly with the applied field in the range 0–2.0 T. This behaviour is typical of simple paramagnets. Above 6 K the corrected molar magnetic susceptibilities of compounds **1–3** follow the Curie–

TABLE 10. UV-Vis spectral data for compounds **1–3** [a]

Compound	λ_{max} (nm) (relative ϵ)
1	236(5.79), 299(6.69), 332(2.83) [b], 402(1.64) [b], 435(3.62), 450(2.77) [b], 490(1.08) [b], 579(1.00)
2	272(6.36), 296(5.75) [b], 330(2.68) [b], 400(1.62) [b], 436(3.62), 500(1.07) [b], 576(1.00)
3	295(11.66), 316(9.07) [c], 358(2.38) [b], 433(1.00)

[a] CH_3CN solution, *ca.* 0.02 mM. [b] Shoulder. [c] Inflection.

Weiss expression, *i.e.* $\chi = C/(T - \theta)$, with small values of θ ($\theta = -2.5$ K for **1**; $\theta = -2.0$ K for **2** and $\theta = +1.5$ K for **3**). The θ values suggest that there is negligible interaction between the unpaired spins of the ions in the solids. Correspondingly, the effective magnetic moments, μ_{eff} [$\mu_{eff} = 2.83\ (\chi T)^{1/2}$], of all three compounds are effectively independent of temperature. The μ_{eff} values of 2.42 and 1.74 μ_B for **2** and **3**, respectively, are very close to the μ_{eff} values of the tetramethylammonium salts of the corresponding metallacarborane anions [5] and consistent with their low spin configurations (d^5 and d^7). This is consistent with the absence of monomeric $ttf^{\cdot+}$ radical cations in the crystal of **2** and **3**. The failure to observe cooperative magnetic behaviour in **2** and **3** is thus not surprising since, according to the extended-McConnell model, cooperative behaviour is only possible in systems where both the cation and anion have unpaired spins [3].

The μ_{eff} of **1**, 3.96 μ_B, is slightly lower than the value of 4.22 μ_B calculated using the formula for two non-interacting spins: $\chi_{total} = \chi_{cation} + \chi_{anion}$; $[(\mu_{eff})_{total}]^2 = [(\mu_{eff})_{cation}]^2 + [(\mu_{eff})_{anion}]^2$. [The spin-only μ_{eff} value of 1.73 μ_B is assumed for $ttf^{\cdot+}$ and the μ_{eff} of 3.85 μ_B for $[Cr(C_2B_9H_{11})_2]^-$ is taken from ref. 5a.]

^{11}B and ^{13}C nuclear magnetic resonance studies of $[Cr(C_2B_9H_{11})_2]^-$ have revealed a small extent of delocalization of the unpaired electron density from Cr to the C_2B_3 bonding face [18]. Thus, for the unpaired spins on $ttf^{\cdot+}$ (primarily localized on the sulfur atoms) [19] and $[Cr(C_2B_9H_{11})_2]^-$ to interact, the distances between the $ttf^{\cdot+}$ sulfur atoms and any atom of the $[Cr(C_2B_3)_2]$ moiety of the chromacarborane must be short enough for significant orbital overlap between the ions to occur. The long Cr $\cdots$ S distances of 5.9 and 6.8 Å in **1** (*vide supra*) are comparable to the Fe $\cdots$ N(TCNE) distances of 5.5–6.5 Å in $[Cp^*_2Fe]^{\cdot+}[TCNE]^{\cdot-}$ which is a bulk ferromagnet below 5 K ($\theta = +30$ K) [2d]. The lack of any significant cooperative behaviour of **1** even at 6 K thus casts doubt on the simple mechanism proposed by Miller and coworkers to explain the spin-coupling between $[Cp^*_2Fe]^{\cdot+}$ and $[TCNE]^{\cdot-}$, since Miller's mechanism involves spin exchange between the Fe atom of $[Cp^*_2Fe]^{\cdot+}$ and the N atoms of $[TCNE]^{\cdot-}$ [2d]. The distances between the $ttf^{\cdot+}$ sulfur atoms and the atoms on the C_2B_3 bonding faces of the chromacarborane are also too long (*vide supra*) for any significant orbital overlap.

3. Conclusions

This study has established that it is possible to synthesize charge transfer salts of metallacarborane sandwich compounds with the radical cation $ttf^{\cdot+}$ that are complementary to those studied by Miller and based on metallocenes. The salts **2** and **3** do not adopt the same packing modes in the crystalline state as that observed in **1**. In **2** and **3**, the $ttf^{\cdot+}$ radical cations are dimerized whereas in **1** the $ttf^{\cdot+}$ ions form layers. This is unusual, since these cations do not usually adopt the latter packing motif. Unlike the Miller compounds the $ttf^{\cdot+}$ ions do not interweave between the sandwich ions, and so the corresponding co-operative magnetic phenomenon is not observed.

4. Experimental details

4.1. General

Tetrathiafulvalene was purchased from Aldrich and used as received. The compounds $[ttf]_3[BF_4]_2$ [8], $Cs[Cr(C_2B_9H_{11})_2]$ [5a], $[Me_4N][Fe(C_2B_9H_{11})_2]$ [5b] and $[Ni(C_2B_9H_{11})_2]$ [5b] were prepared following reported procedures. Organic solvents were of reagent grade and were dried by published procedures [20] and distilled under N_2. The solvents were vacuum-degassed before use. All reactions were routinely carried out under N_2 by standard Schlenk techniques.

4.2. Synthesis of $[ttf]^{\cdot+}Cl^-$

A solution of $[ttf]_3[BF_4]_2$ (0.080 g, 0.11 mmol) in warm (*ca.* 70°C) CH_3CN (40 cm^3) was filtered under N_2 into a flask containing a magnetically stirred solution of $[Et_4N]Cl \cdot H_2O$ (0.056 g, 0.30 mmol) in CH_3CN (18 cm^3) at room temperature. A purple precipitate formed immediately. The precipitate was filtered off from the yellow solution and washed with four 10 cm^3 portions of cold CH_3CN then dried *in vacuo*. The solid was then extracted with a minimum amount of warm (*ca.* 70°C) deionized water. The water was removed from the filtered extract *in vacuo*, leaving a purple microcrystalline residue, which was washed with another 2 cm^3 of cold CH_3CN and dried *in vacuo*. Yield: 0.039 g, 79%. Anal. Found: C, 30.17; H, 1.32. $C_6H_4ClS_4$ calc.: C, 30.08; H, 1.68%.

4.3. Synthesis of $[ttf]^{\cdot+}[Cr(C_2B_9H_{11})_2]^-$ (1)

A warm (*ca.* 70°C) solution of $[ttf]^{\cdot+}Cl$ (0.028 g, 0.12 mmol) in deionized water (40 cm^3) was filtered under N_2 into a flask containing a magnetically stirred solution of $Cs[Cr(C_2B_9H_{11})_2]$ (0.050 g, 0.11 mmol) in boiling deionized water (20 cm^3). A dark brown powdery precipitate formed immediately. The mixture was cooled to room temperature and the precipitate filtered off, and washed with cold deionized water (2 × 40 cm^3). Recrystallization from acetone/ethanol mixture yielded 0.043 g (75%) of **1** as black shiny microcrystals.

Anal. Found: C, 23.16; H, 5.03; Cr, 9.94. $C_{10}H_{26}B_{18}CrS_4$ calc.: C, 23.05; H, 5.03; Cr, 9.98%.

4.4. Synthesis of $[ttf]^{\cdot+}[Fe(C_2B_9H_{11})_2]^-$ (2)

A solution of $[Me_4N][Fe(C_2B_9H_{11})_2]$ (0.050 g, 0.13 mmol) in acetone was loaded on to a column (2 cm × 32 cm) of Dowex 50 cation-exchange resin (previously converted to the Na^+ form by soaking in 3 M aqueous NaCl solution overnight). The column was eluted first with 10 cm^3 of H_2O/acetone (3:2) mixture and then with deionized water. The volume of the eluant was reduced to 20 cm^3 *in vacuo* and the resulting red solution was added to a filtered solution of $ttf^{\cdot+}Cl^-$ (0.030 g, 0.13 mmol) in water (35 cm^3) with constant agitation. The fine reddish-brown precipitate that formed immediately was collected by centrifugation and washed with 2 × 40 cm^3 of cold deionized water. Recrystallization from acetone/ethanol afforded 0.038 g (58%) of **2** as black shiny microcrystals. Anal. Found: C, 23.24; H, 5.18; Fe, 10.86. $C_{10}H_{26}B_{18}FeS_4$ calc.: C, 22.90; H, 5.00; Fe, 10.65%.

4.5. Synthesis of $[ttf]^{\cdot+}[Ni(C_2B_9H_{11})_2]^-$ (3)

A mixture of $[Ni(C_2B_9H_{11})_2]$ (0.029 g, 0.090 mmol) and ttf (0.019 g, 0.091 mmol) was dissolved in 5 cm^3 of CH_2Cl_2 in a Schlenk tube. An equal volume of n-hexane was then added. The resulting chrome-yellow solution was filtered under N_2 into another Schlenk tube. Slow evaporation of the solution under a N_2 stream resulted in the formation of large black, shiny crystals of **3** after 1 day. Yield: 0.026 g, 55%. Anal. Found: C, 22.86; H, 4.97. $C_{10}H_{26}B_{18}NiS_4$ calc.: C, 22.76; H, 4.97%.

4.6. Physical measurements

Infrared spectra were recorded on a Perkin-Elmer 1720 infrared Fourier transform spectrometer on KBr pellets. A Perkin-Elmer lambda 2 UV/VIS spectrophotometer was used to record the electronic spectra. Magnetic susceptibility measurements were performed in the ranges $6 \leq T < 296$ K (for compounds **1** and **2**) and $6 \leq T \leq 185$ K (for compound **3**) using a Cryogenic Consultants SCU 500 SQUID susceptometer, under magnetic field strengths of 1.8, 0.3 and 3.0 T, respectively. The susceptibilities were corrected for the diamagnetism of the quartz sample bucket and that of the constituent atomic cores by fitting the susceptibility data to the expression $\chi^{-1} = (T-\theta)[C + K(T-\theta)]^{-1}$, where K comprises the total diamagnetism and any temperature-independent paramagnetism of the sample.

4.7. Crystal structure determinations

The crystal and refinement data for compounds **1–3** are summarized in Table 1. The crystals were prepared as described in Section 2, and were either mounted at the end of a glass fibre (compound **1**) or sealed in Lindemann capillaries (compounds **2** and **3**).

The structure of **1** was solved by the heavy atom method. Positional and anisotropic thermal parameters for non-hydrogen atoms were refined by the full-matrix least-squares method. Hydrogen atoms of the $ttf^{\cdot+}$ molecule were introduced in calculated positions and refined isotropically. Hydrogen atoms on the carborane cages were located by difference syntheses and refined with the bond length constraints C–H = 0.960 ± 0.002 Å and B–H = 1.080 ± 0.002 Å and assigned isotropic thermal parameters $U(H) = 1.2\ U_{eq}(C, B)$. All calculations were performed on 386 and 486 PCs using the SHELXTL PLUS (PC version) software package [21].

The iron and sulfur atomic positions for **2** were located by direct methods. All the remaining atoms, including the hydrogen atoms, were located by subsequent difference syntheses. The positional parameters of the hydrogen atoms were not refined but a common isotropic temperature factor was refined for each group of hydrogen atoms, *i.e.* the ttf hydrogens were refined separately from the hydrogen atoms of the carborane cage. All the non-hydrogen atoms were refined anisotropically using the full-matrix least-squares method. Calculations were performed on a Micro Vax 3000 computer in the Chemical Crystallography Laboratory using the Oxford CRYSTALS system [22].

The structure of **3** was solved by direct methods. The refinement procedure was identical to that used for **1**.

For all three compounds, complete lists of bond lengths and angles and tables of thermal parameters and hydrogen atom coordinates have been deposited at the Cambridge Crystallographic Data Centre.

References

1 (a) C. Bellitto, M. Bonamico, V. Fares, P. Imperatori and S. Patrizio, *J. Chem. Soc., Dalton Trans.*, (1989) 719; (b) D. Attanasio, C. Bellitto, M. Bonamico, V. Fares and P. Imperatori, *Gazz. Chim. Ital., 121* (1991) 155; (c) S. Triki, L. Ouahab, J.-F. Halet, O. Pena, J. Padiou, D. Grandjean, C. Garrigou-Lagrange and P. Delhaes, *J. Chem. Soc., Dalton Trans.*, (1992) 1217; (d) A. Penicaud, P. Batail, C. Perrin, C. Coulon, S.S.P. Parkin and J.B. Torrance, *J. Chem. Soc., Chem. Commun.*, (1987) 330; (e) V. Gama, R.T. Henriques, G. Bonfait, M. Almeida, A. Meetsma, S. van Smaalen and J.L. de Boer, *J. Am. Chem. Soc., 114* (1992) 1986; (f) F. Wudl, D.E. Schafer, W.M. Walsh, Jr., L.W. Rupp, F.J. DiSalvo, J.V. Waszczak, M.L. Kaplan and G.A. Thomas, *J. Chem. Phys., 66* (1977) 377.

2 (a) J.S. Miller, A.J. Epstein and W.M. Reiff, *Acc. Chem. Res., 21* (1988) 114; (b) W.E. Broderick, J.A. Thompson, E.P. Day and B.M. Hoffman, *Science, 249* (1990) 401; (c) J.S. Miller, R.S. McLean, C. Vazquez, J.C. Calabrese, F. Zuo and A.J. Epstein, *J. Mater. Chem., 3* (1993) 215; (d) J.S. Miller, J.C. Calabrese, H. Rommelmann, S.R. Chittipeddi, J.H. Zhang, W.M. Reiff and

A.J. Epstein, *J. Am. Chem. Soc., 109* (1987) 769; (e) I.S. Jacobs, H.-R. Hart, Jr., L.V. Interrante, J.W. Bray, J.S. Kasper, G.D. Watkins, D.E. Prober, W.P. Wolf and J.C. Bonner, *Physica B, 86–88* (1977) 655; (f) J.S. Miller, R.S. McLean, C. Vazquez, G.T. Yee, K.S. Narayan and A.J. Epstein, *J. Mater. Chem., 1* (1991) 479; (g) W.E. Broderick, J.A. Thompson and B.M. Hoffman, *Inorg. Chem., 30* (1991) 2958.

3 (a) J.S. Miller, A.J. Epstein and W.M. Reiff, *Chem. Rev., 88* (1988) 201; (b) J.S. Miller and A.J. Epstein, *J. Am. Chem. Soc., 109* (1987) 3850.

4 (a) C. Kollmar and O. Kahn, *J. Am. Chem. Soc., 113* (1991) 7987; (b) C. Kollmar, M. Couty and O. Kahn, *J. Am. Chem. Soc., 113* (1991) 7994; (c) C. Kollmar and O. Kahn, *J. Chem. Phys., 96* (1992) 2988.

5 (a) H.W. Ruhle and M.F. Hawthorne, *Inorg. Chem., 7* (1968) 2279; (b) M.F. Hawthorne, D.C. Young, T.D. Andrews, D.V. Howe, R.L. Pilling, A.D. Pitts, M. Reintjes, L.F. Warren Jr. and P.A. Wegner, *J. Am. Chem. Soc., 90* (1968) 879; (c) L.F. Warren, Jr. and M.F. Hawthorne, *J. Am. Chem. Soc., 92* (1970) 1157; (d) C.G. Salentine and M.F. Hawthorne, *Inorg. Chem., 15* (1976) 2872; (e) L.F. Warren, Jr. and M.F. Hawthorne, *J. Am. Chem. Soc., 90* (1968) 4823.

6 R.N. Grimes, in G. Wilkinson, F.G.A. Stone and E.W. Abel (eds.), *Comprehensive Organometallic Chemistry*, Pergamon, Oxford, 1982, Vol. 1, Chap. 5.5, p. 459.

7 J.M. Forward, *D. Phil. Thesis*, University of Oxford, 1993.

8 F. Wudl, *J. Am. Chem. Soc., 97* (1975) 1962.

9 D. St. Clair, A. Zalkin and D.H. Templeton, *Inorg. Chem., 10* (1971) 2587.

10 K. Yakushi, S. Nishimura, T. Sugano, H. Kuroda and I. Ikemoto, *Acta Crystallogr., Sect. B, 36* (1980) 358.

11 H.C. Kang, S.S. Lee, C.B. Knobbler and M.F. Hawthorne, *Inorg. Chem., 30* (1991) 2024.

12 F.V. Hansen, R.G. Hazell, C. Hyatt and G.D. Stucky, *Acta Chem. Scand., 27* (1973) 1210.

13 D.M.P. Mingos, M.I. Forsyth and A.J. Welch, *J. Chem. Soc., Chem., Commun.,* (1977) 605.

14 D.M.P. Mingos and A.L. Rohl., *J. Chem. Soc., Dalton Trans.,* (1991) 3419.

15 R. Bozio, I. Zanon, A. Girlando and C. Pecile, *J. Chem. Phys., 71* (1979) 2282.

16 J.B. Torrance, B.A. Scott, B. Welber, F.B. Kaufman and P.E. Seiden, *Phys. Rev., 19B* (1979) 730.

17 D.L. Coffen, J.Q. Chambers, D.R. Williams, P.E. Garrett and N.D. Canfield, *J. Am. Chem. Soc., 93* (1971) 2258.

18 R.J. Wiersema and M.F. Hawthorne, *J. Am. Chem. Soc., 96* (1974) 761.

19 J.P. Lowe, *J. Am. Chem. Soc., 102* (1980) 1262.

20 A.J. Gordon and R.A. Ford, *The Chemist's Companion: A Handbook of Practical Data, Techniques and References*, Wiley-Interscience, New York, 1972.

21 G.M. Sheldrick, SHELXTL PC, Version 4.2, Siemens Analytical X-Ray Instruments Inc, 1990.

22 J.R. Carruthers and D.J. Watkin, *Acta Crystallogr., Sect. A, 35* (1979) 698.